applied sciences

MDPI

Article

Characteristics and Predictive Significance of Spatio-Temporal Space Images of $M \geq 4.0$ Seismic Gaps on the Southeastern Margin of the Tibetan Plateau

Xiaoyan Zhao, Youjin Su * and Guangming Wang

Yunnan Earthquake Agency, Kunming 650224, China; zhaoxiaoyan@seis.ac.cn (X.Z.); gmwang@whu.edu.cn (G.W.)
* Correspondence: suyoujin@seis.ac.cn; Tel.: +86-871-6574-7052

Abstract: In the present study, seismic gaps were identified as periods with no occurrence of $M \geq 4.0$ earthquake over d$T \geq 400$ days. After examining all records in the Sichuan–Yunnan–Tibet–Qinghai junction area on the southeastern margin of the Tibetan Plateau in 1970–2022, a total of six $M \geq 4.0$ seismic gaps were identified. Spatio-temporal images of the seismic gaps had similar characteristics and demonstrated spatial overlapping and statistical significance. The quiet periods of the six seismic gaps included 419–777 days (approximately 580 days on average). The semi-major-axis and semi-minor-axis lengths were in the 880–1050 km (approximately 987 km on average) and 500–570 km (about 533 km on average) ranges, respectively. Case analysis results revealed that the images of $M \geq 4.0$ seismic gaps were of high significance in predicting $M \geq 6.7$ strong earthquakes in the region, and they could be used as a predictive index on a time scale of about 1–0.5 years or less.

Keywords: southeastern margin of the Tibetan Plateau; $M \geq 4.0$ seismic gap; $M \geq 6.7$ strong earthquake; predictive index

check for updates

Citation: Zhao, X.; Su, Y.; Wang, G. Characteristics and Predictive Significance of Spatio-Temporal Space Images of $M \geq 4.0$ Seismic Gaps on the Southeastern Margin of the Tibetan Plateau. *Appl. Sci.* **2023**, *13*, 7937. https://doi.org/10.3390/app13137937

Academic Editors: Luciano Zuccarello and Janire Prudencio

Received: 4 June 2023
Revised: 29 June 2023
Accepted: 3 July 2023
Published: 6 July 2023

1. Introduction

Seismic gap images have increasingly attracted the attention of researchers in seismic activity and earthquake prediction theory and methodology research [1–15]. Mogi [2] proposed two types of seismic gaps. The first type represents large earthquake rupture gaps in seismic zones along plate boundaries or intra-plate tectonic boundaries, whereas the second represents a phenomenon where minor earthquake activity at and around the hypocenter decreases suddenly or showcases a lull before a strong earthquake. In China, seismologists normally refer to the second type as precursory seismic or seismogenic gaps, and they provide insights that could facilitate medium and short-term prediction of earthquakes [4,5].

Based on routine earthquake monitoring, from the M4.2 earthquake in Luhuo, Sichuan on 3 June 2020 to the M5.5 earthquake in Ninglang, Yunnan on 2 January 2022, there was a $M \geq 4.0$ seismic gap image with a quiet period of approximately 577 days in the Sichuan–Yunnan–Tibet–Qinghai junction area on the southeastern margin of the Tibetan Plateau. The gap was terminated by the M5.5 earthquake in Ninglang on 2 January 2022. In addition, approximately eight months later, on 5 September 2022, a strong earthquake of 6.8 magnitude occurred within the gap in Luding, Sichuan.

In the present study, attempts are made to answer the following questions. Have similar seismic gap images been observed frequently in the region in the past? In other words, do such images emerge repeatedly and are they statistically significant when all past records of the region are examined? In addition, are there always strong earthquakes after the gap is terminated, and could the images give valid predictions of subsequent strong earthquakes?

2. Study Area and Earthquake Catalog

The study area is located at 24°–36° N, 92°–106° E on the southeastern margin of the Tibetan Plateau. It covers mainly western Sichuan, north-central Yunnan, eastern Tibet, and southern Qinghai. According to the division scheme of tectonically active blocks in China [16,17], the study area mainly includes the Sichuan-Yunnan block, the Qiangtang block, and the Bayan Har block. Fault zones, such as the Karakorum-Jiali fault zone, the Jinshajiang-Honghe fault zone, the Mani-Yushu-Xianshuihe fault zone, the Zemuhe-Anninghe-Xiaojiang fault zone, the Longmenshan fault zone, and the Kunlun-Maqin fault zone, are present in the study area. There are complex geological structures, vigorous modern tectonic activity, and frequent strong earthquakes in the region. In particular, the Sichuan-Yunnan block is divided into two: the western Sichuan block and the central Yunnan block [18,19]. The slip rate of the former is 5.4–7.6 mm/a, while that of the latter is 3 mm/a approximately. The modern tectonic movement of the western Sichuan block is approximately twice as rapid as that of the central Yunnan block. The distributions of tectonic blocks and $M \geq 6.7$ earthquakes in the study area in 1970–2022 are illustrated in Figure 1. Since 1970, strong earthquakes ($M \geq 6.7$) have mainly occurred in the fault zones along the boundary of the western Sichuan block (the Xianshuihe fault zone and the Jinshajiang fault zone), as well as the Longmenshan fault zone. The earthquake catalog adopted is the National Small Earthquake Catalog published by the China Earthquake Networks Center (it includes all $M_L \geq 1.0$ earthquakes in China since 1970). The Richter local magnitude scale is used in the catalog (in M_L); thereafter, it is uniformly represented by M in this paper. A complete and reliable earthquake catalog is important for seismicity analysis. Previous research [20–22] has indicated that the records for $M \geq 3.0$ earthquakes in the Sichuan-Yunnan region since 1970 and those in the Tibetan Plateau since 1980 are complete. Hence, since 1970 $M \geq 4.0$ earthquakes in the study area can ensure their completeness. Figure 2a–c presents the epicenter distribution, magnitude–frequency graph, and M-t curve of $M \geq 4.0$ earthquakes in the study area in 1970–2022.

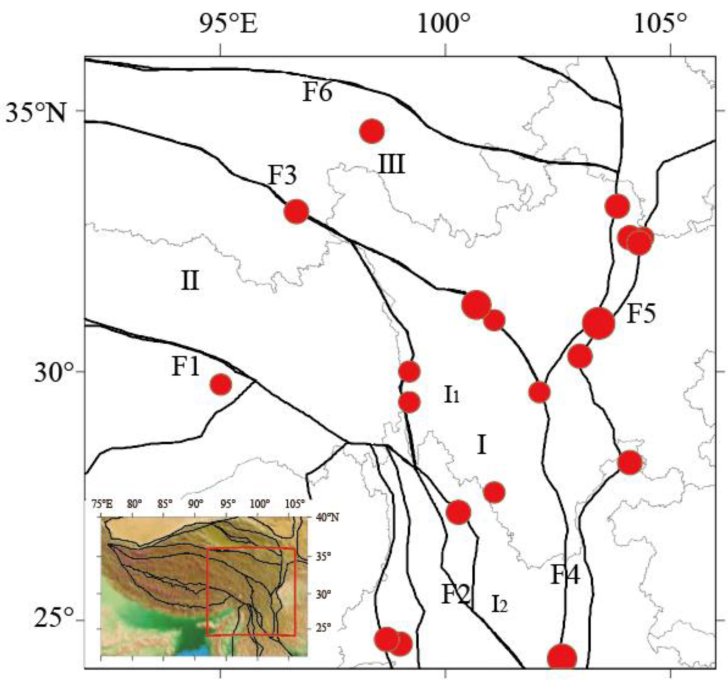

Figure 1. Distribution of tectonic blocks and $M \geq 6.7$ earthquakes in the study area in 1970–2022. Red circles denote $M \geq 6.7$ earthquakes in 1970−2022, while black lines are the boundaries of the tectonic blocks. I: Sichuan–Yunnan block (I_1: western Sichuan block, I_2: central Yunnan block), II: Qiangtang block, III: Bayan Har block. F1: Karakorum-Jiali fault zone, F2: Jinshajiang–Honghe fault zone, F3: Mani–Yushu–Xianshuihe fault zone, F4: Zemuhe–Anninghe–Xiaojiang fault zone, F5: Longmenshan fault zone, F6: Kunlun–Maqin fault zone.

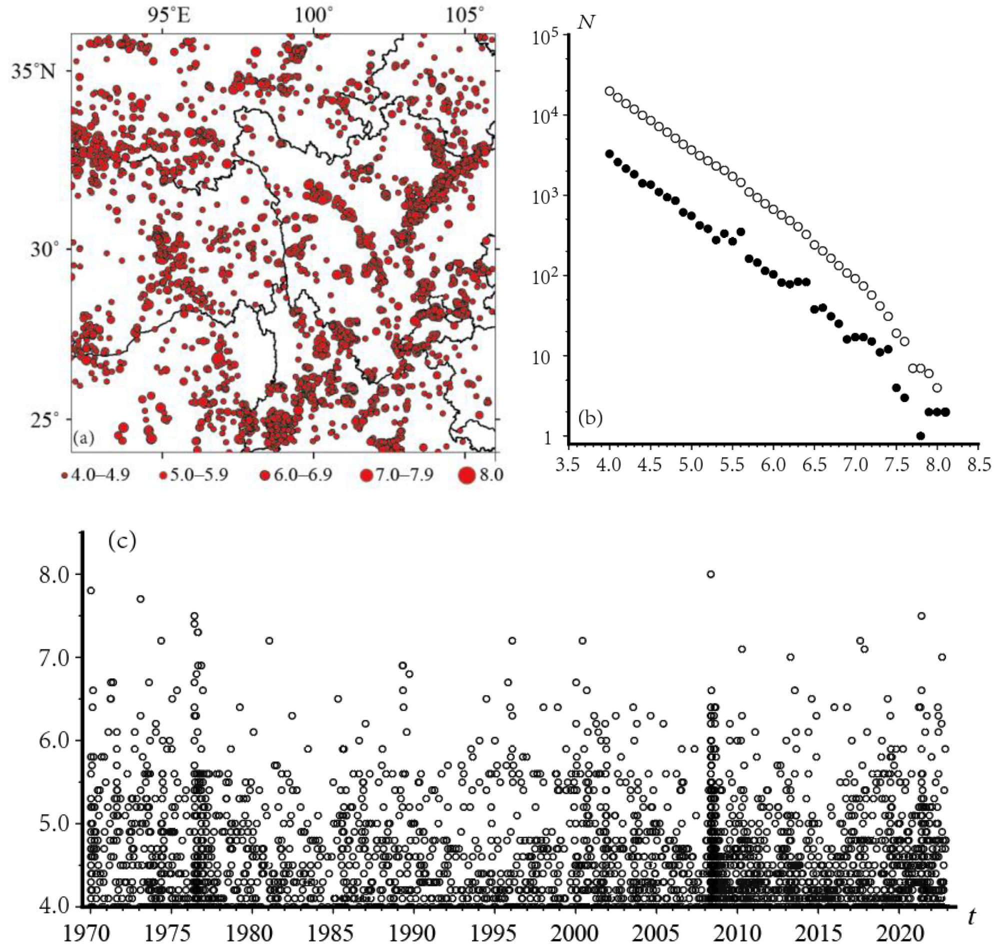

Figure 2. (**a**) The epicenter distribution, (**b**) incremental (solid black circles) and cumulative (hollow black circles) frequency-magnitude distributions graph, and (**c**) the M-t curve of $M \geq 4.0$ earthquakes in the study area from 1970 to 2022.

3. Spatio-Temporal Images of Seismic Gaps

Images of the $M \geq 4.0$ seismic gap between the M4.2 earthquake in Luhuo, Sichuan on 3 June 2020, and the M5.5 earthquake in Ninglang, Yannan, on 2 January 2022 (hereafter referred to as No. 6 gap), are taken as the reference (Figure 3f). A seismic gap is defined as a quiet period lasting d$T \geq 400$ days with no occurrence of $M \geq 4.0$ earthquakes. All records since 1970 in the study area were studied to identify other five similar $M \geq 4.0$ seismic gap images in history (Figure 3a–e). They are described as follows. No. 1 seismic gap: between the M5.5 earthquake in Rangtang, Sichuan on 8 November 1970, to the M5.2 earthquake in Kangding, Sichuan on 8 April 1972, with a 517-day quiet period with no $M \geq 4.0$ earthquake occurrence. No. 2 seismic gap: from the M4.7 earthquake in Yanyuan, Sichuan on 13 August 1986 to the M5.5 earthquake in Ninglang, Yunnan, on 10 January 1988, with no occurrence of $M \geq 4.0$ earthquakes for approximately 514 days. No. 3 seismic gap: between the M4.2 earthquake in Ninglang, Yunnan on 17 December 1993 and the M7.0 earthquake in Lijiang, Yunnan on 3 February 1996, with no occurrence of $M \geq 4.0$ earthquakes for approximately 777 days. No. 4 seismic gap: from the M4.3 earthquake in Mangkang, Tibet on 13 July 2007, to the M4.2 earthquake in Ganzi, Sichuan, on 6 September 2008, with an approximate 419-day quiet period with no $M \geq 4.0$ earthquake occurrence. No. 5 seismic gap: between the M4.6 earthquake in Shangri-La, Yunnan, on 29 November 2013, and the M4.2 earthquake in Zuogong, Tibet on 3 October 2015, with a roughly 673-day quiet period. The spatial dimensions and semi-major-axis directions (spatial distributions) of the six seismic gaps are similar. Their semi-major axes lie in the NNW direction.

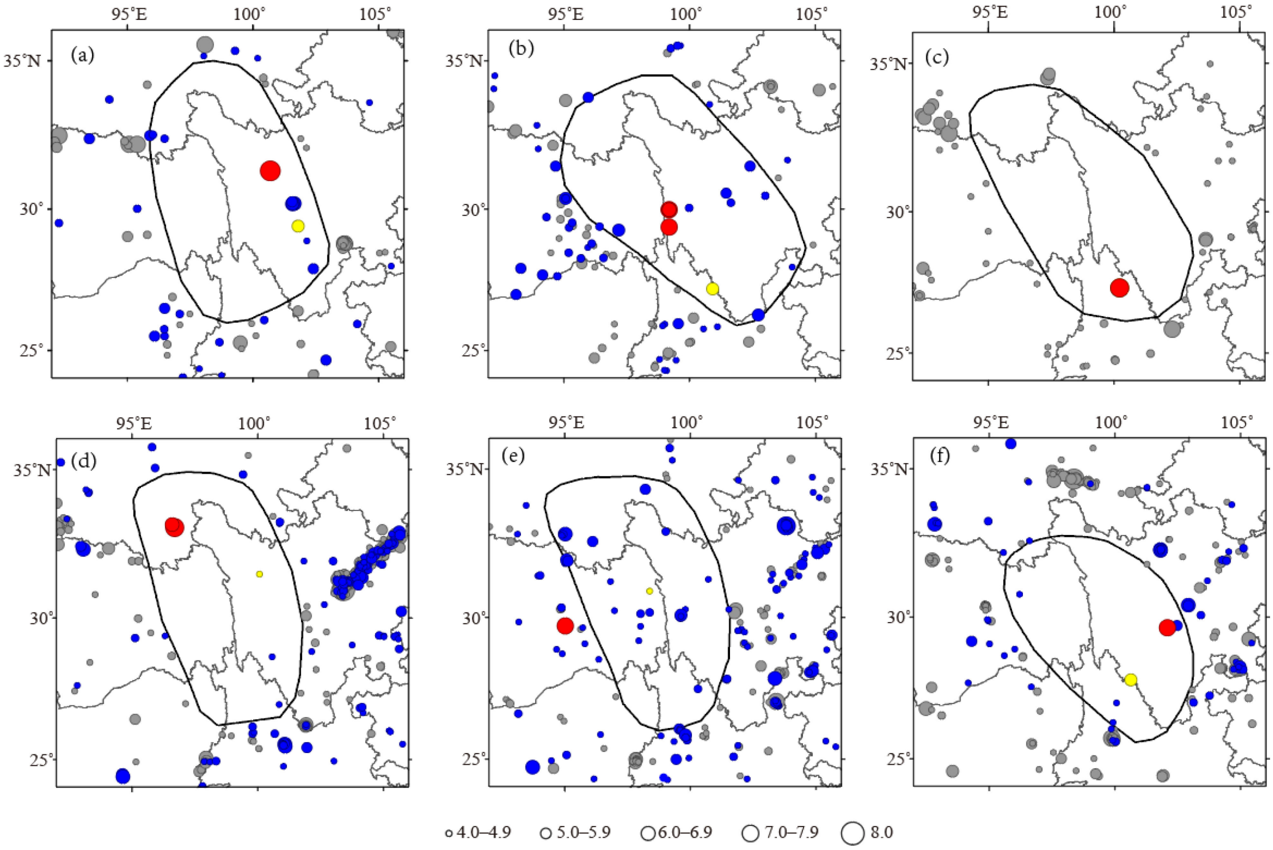

Figure 3. Spatial images of the six M ≥ 4.0 seismic gaps in the study area from 1970 to 2022. Gray circles: earthquakes surrounding the spatial location of the gap; yellow circles: earthquakes ending the gaps; blue circles: earthquakes in the periods between the ends of the gaps and before the strong earthquakes; red circles: strong earthquakes corresponding to the seismic gaps; black thick lines: the margins of six seismic gaps.

To evaluate the impact of the lower magnitude limit on seismic gap identification, earthquake interval graphs (dT-t) with three different lower limits, i.e., $M \geq 3.7$, $M \geq 4.0$, and $M \geq 4.3$, were plotted separately for each seismic gap (Green lines: $M \geq 3.7$; Red lines: $M \geq 4.0$; Blue lines: $M \geq 4.3$). In the plots, threshold lines of dT = 400 days (Black dashed lines)and lines indicating the six time variances of the $M \geq 4.0$ interval times (6σ, Black solid lines) are added (Figure 4a–f). As shown in the figures, for the six seismic gaps (No. 1–No. 6), there are no notable patterns observed in the interval graphs for $M \geq 3.7$ earthquakes. However, obvious patterns are observed for $M \geq 4.0$ or $M \geq 4.3$ earthquake intervals. The results suggest that $M = 4.0$ is the lower limit for identifying seismic gap images.

No. 1 seismic gap (Figure 4a): The quiet period with no occurrence of $M \geq 4.0$ earthquakes lasts approximately 517 days, which is significantly longer than the dT = 400-day and 6σ = 350-day thresholds. The $M \geq 4.0$ and $M \geq 4.3$ earthquake interval images are completely consistent (the quiet period with no occurrence of $M \geq 4.3$ earthquakes is 517 days).

No. 2 seismic gap (Figure 4b): The quiet period with no occurrence of $M \geq 4.0$ earthquakes is approximately 514 days, which is remarkably longer than the dT = 400-day and 6σ = 240-day thresholds. Furthermore, the $M \geq 4.0$ and $M \geq 4.3$ earthquake interval images are perfectly consistent (the quiet period with respect to $M \geq 4.3$ earthquakes is 514 days).

No. 3 seismic gap (Figure 4c): There are no $M \geq 4.0$ earthquakes for approximately 777 days. This is considerably longer than the dT = 400 day and 6σ 370 day thresholds. The $M \geq 4.0$ and $M \geq 4.3$ earthquake interval images are basically consistent (the quiet period with respect to $M \geq 4.3$ earthquakes is approximately 835 days, between the M4.8

earthquake in Mangkang, Tibet on 19 October 1993, to the M7.0 earthquake in Lijiang, Yunnan, on 3 February 1996).

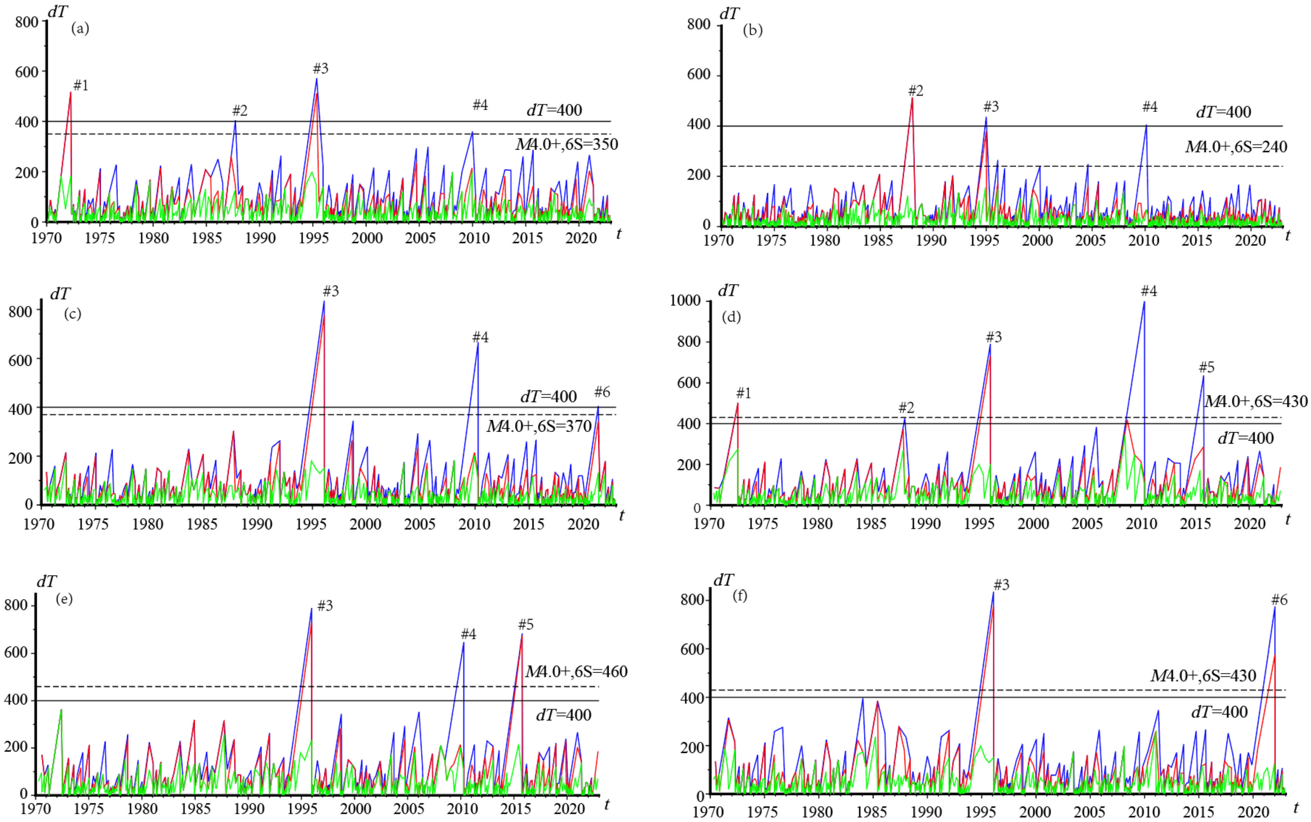

Figure 4. $M \geq 3.7$, $M \geq 4.0$, and $M \geq 4.3$ earthquake interval graphs for the six seismic gaps in 1970–2022. Green lines: $M \geq 3.7$; Red lines: $M \geq 4.0$; Blue lines: $M \geq 4.3$; Black dashed lines: threshold lines of dT = 400 days; Black solid lines: threshold lines of six time variances of the $M \geq 4.0$ interval times; #: Number of the seismic gap.In the earthquake interval graph for the No. 1 seismic gap (Figure 4a), obvious patterns are not only noted for the No. 1 gap, but also those for No. 2–No. 4 are prominent (#2, #3, and #4 in Figure 4a). Similarly, in the graph for the No. 2 gap, indicative patterns for the No. 3 and No. 4 gaps are observed (#3 and #4 in Figure 4b). In the graph for the No. 3 gap, patterns indicative of No. 4 and No. 6 gaps are noted (#4 and #6 in Figure 4c). In the graph for the No. 4 seismic gap, patterns for No. 1–No. 3 and No. 5 gaps are found (#1, #2, #3, and #5 in Figure 4d). In the graph for the No. 5 gap, patterns for No. 3 and No. 4 are noted (#3 and #4 in Figure 4e). Finally, in the interval graph for the No. 6 seismic gap, patterns for the No. 3 gap are found (#3 in Figure 4f). The results demonstrated that the six seismic gaps have good spatial overlapping. In particular, the No. 1 and No. 4 seismic gaps demonstrate the best spatial overlapping with other gaps.

No. 4 seismic gap (Figure 4d): The quiet period with no occurrence of $M \geq 4.0$ earthquakes is approximately 419 days, which is longer than the dT = 400-day threshold but less than the 6σ = 430-day threshold. However, the $M \geq 4.3$ earthquake interval images are prominent (the quiet period with respect to $M \geq 4.3$ earthquakes is 1005 days, from the M4.3 earthquake in Mangkang, Tibet on 13 July 2007, to the M4.8 earthquake in Yushu, Qinghai, on 14 April 2010).

No. 5 seismic gap (Figure 4e): There are no $M \geq 4.0$ earthquakes for approximately 673 days. This is notably longer than the dT = 400 day and 6σ 460 day thresholds. The $M \geq 4.0$ and $M \geq 4.3$ earthquake interval images are basically consistent (The quiet period with no occurrence of $M \geq 4.3$ earthquakes is approximately 682 days, between the M4.6 earthquake in Shangri-La, Yunnan, on 29 November 2013, to the M5.2 earthquake in Maduo, Qinghai, on 12 October 2015).

No. 6 seismic gap (Figure 4f): The quiet period with no occurrence of $M \geq 4.0$ earthquakes is approximately 577 days, which is significantly longer than the dT = 400-day and 6σ = 430-day thresholds. Yet, the $M \geq 4.3$ earthquake interval images are prominent (the corresponding quiet period is 774 days, from the M4.5 earthquake in Muli, Sichuan, on 19 November 2019, to the M5.5 earthquake in Ninglang, Yunnan, on 2 January 2022).

In short, the six time variances of the $M \geq 4.0$ earthquake interval times (6σ) lie between 240 and 460 days (with an average of 380 days). The values are basically equivalent to the defined threshold of dT = 400 days (excluding the relatively large difference for the No. 2 seismic gap). In other words, the seismic gap identification results are basically similar regardless of whether the six time variance line or the dT threshold line is used. This further statistically confirms the objectivity and significance of the images of the six seismic gaps.

By overlaying the $M \geq 4.0$ earthquake interval curves of the six seismic gaps (Figure 5), the temporal images of the six gaps can be clearly identified (the temporal image signals become stronger after overlaying). In Figure 5, the corresponding earthquake of each gap is also marked (more details in later sections).

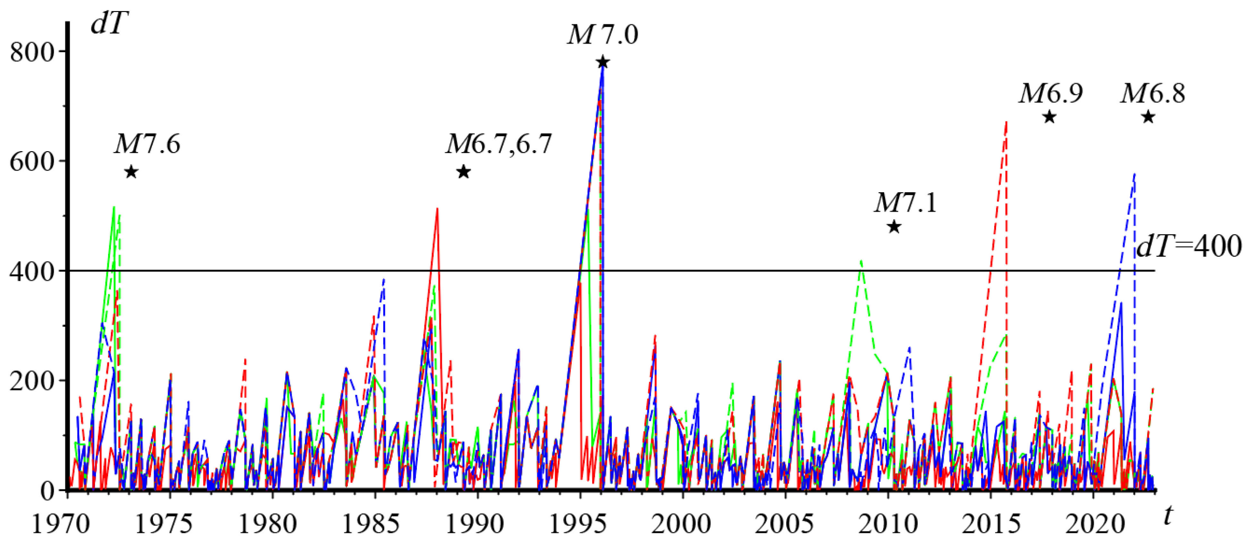

Figure 5. Combined $M \geq 4.0$ earthquake intervals of the six seismic gaps. Green solid line: No. 1 seismic gap; Red solid line: No. 2 seismic gap; Blue solid line: No. 3 seismic gap. Green dotted line: No. 4 seismic gap; Red dotted line: No. 5 seismic gap; Blue dotted line: No. 6 seismic gap.

4. Case Analysis

The first $M \geq 6.7$ earthquake, which occurs inside or at the margin of the spatial location of a seismic gap right after the end of the gap, is defined as the earthquake corresponding to the gap. Table 1 lists the characteristic parameters of the spatio-temporal images of the six seismic gaps and the corresponding $M \geq 6.7$ earthquakes. Figure 6 shows the spatial distributions of the gaps and those of their corresponding earthquakes.

According to Table 1 and Figure 6, after each seismic gap ended, $M \geq 6.7$ earthquakes occurred either inside or at the margin of its spatial location. The correspondence rate is 100%. More specifically, five earthquakes took place within the spatial location of the gap (83%) while one was at the margin (17%). The quiet periods of the six seismic gaps are 419–777 days (about 14–26 months), with an average of 580 days (19 months approximately). The major-semi-axis and semi-minor-axis lengths of the gaps are in the 880–1050 km (approximately 987 km on average) and 500–570 km (about 533 km on average) ranges, respectively. The interval times between the ends of the gaps and the corresponding earthquakes are 0–776 days (about 0–26 months), with an average of 395 days (13 months).

Table 1. Characteristic parameters of the spatio-temporal images of the six seismic gaps and the corresponding $M \geq 6.7$ earthquakes.

Earthquake ID	Quiet Period $T1$ (Day/Month)	Semi-Major-Axis Length/Semi-Minor-Axis Length (km)	Earthquakes Marking the Beginning and End of the Seismic Gap	Corresponding Earthquake	Quiet Period $T2$ (Day/Month)
No. 1	517/17	960/570	M5.5 earthquake in Rangtang on 8 November 1970~M5.2 earthquake in Kangding on 8 April 1972	M7.6 earthquake in Luhuo on 6 February 1973	302/10
No. 2	514/17	1030/550	M4.7 earthquake in Yanyuan on 13 August 1986~M5.5 earthquake in Ninglang on 10 January 1988	M6.7 earthquake in Batang on 16 April 1989 *	459/15
No. 3	777/26	1050/540	M4.2 earthquake in Ninglang on 17 December 1993~M7.0 earthquake in Lijiang on 3 February 1996	M7.0 earthquake in Lijiang on 3 February 1996	0/0
No. 4	419/14	990/500	M4.3 earthquake in Mangkang on 13 July 2007 ~M4.2 earthquake in Ganzi on 6 September 2008	M7.1 earthquake in Yushu on 14 April 2010	586/20
No. 5	673/22	1010/520	M4.6 earthquake in Shangri-La on 29 November 2013~M4.2 earthquake in Zuogong on 3 October 2015	M6.9 earthquake in Milin on 18 November 2017	776/26
No. 6	577/19	880/520	M4.2 earthquake in Luhuo on 3 June 2020~M5.5 earthquake in Ninglang on 2 January 2022	M6.8 earthquake in Luding on 5 September 2022	246/8
Average	580/19	987/533			395/13

Interval time $T2$: the time between the end of the seismic gap and the corresponding earthquake. * indicates earthquake swarm.

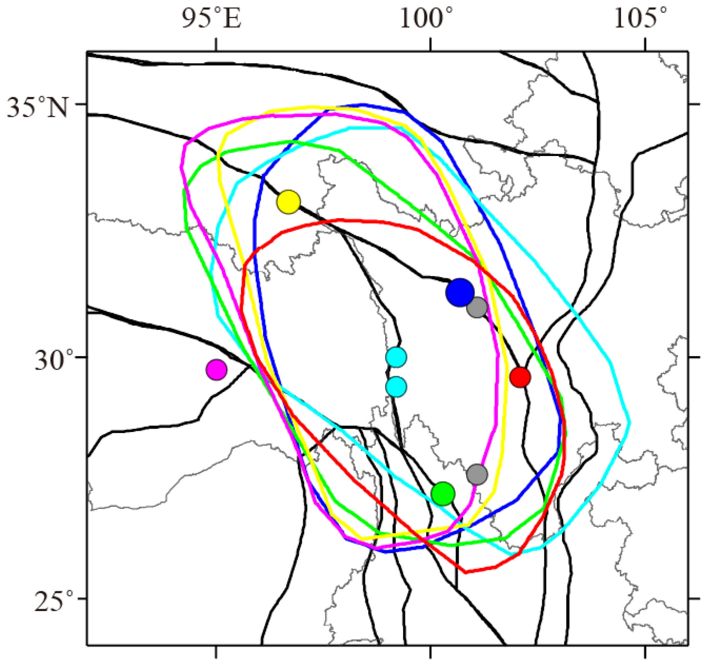

Figure 6. Distributions of $M \geq 6.7$ earthquakes and earthquakes corresponding to the six seismic gaps in the western Sichuan block in 1970–2022. Gray circles: earthquakes with no seismic gap images. Blue, cyan, green, yellow, pink, and red lines and circles: No. 1–6 seismic gaps and their corresponding earthquakes.

Apart from that of the No. 5 gap, the corresponding earthquakes of the other five seismic gaps (No. 1–4 and No. 6) all occurred within the spatial location of the gaps. They were concentrated at the boundary of the western Sichuan block, namely the Xianshuihe fault zone and the Jinshajiang fault zone. A total of seven $M \geq 6.7$ earthquakes (earthquake episodes) occurred within the western Sichuan block or at its boundary in 1970–2022, whereas $M \geq 4.0$ seismic gap images are noted before five of the earthquakes (earthquake episodes) (71%).

The results demonstrate that the occurrence of $M \geq 4.0$ seismic gap images in the region is always followed by that of $M \geq 6.7$ earthquakes, with a correspondence rate of 100%. Meanwhile, the occurrence of $M \geq 4.0$ seismic gap images before that of $M \geq 6.7$ earthquakes is 71%. Hence, more attention should be placed on the $M \geq 4.0$ seismic gap images in the region because they may be of high predictive significance. Nevertheless, further research and discussion are required on how they can be applied in actual earthquake prediction.

Occurrence time prediction: If the $M \geq 4.0$ seismic gap identification threshold, i.e., $T0$ = 400 days, is adopted as the start time for earthquake occurrence time T prediction, parameters $T1$ (quiet period) and $T2$ (time interval between the end of the seismic gap and the corresponding earthquake) in Table 1 can be used to calculate the following: $T = T1 + T2–T0$ (days). The results for No. 1–6 gaps are 419, 573, 377, 605, 1049, and 423 days. The results for the No. 5 seismic gap (1049 days/approximately 35 months) are relatively larger than those for the other five gaps (377–605 days/13–20 months, with an average of 479 days/16 months).

Because the results for the No. 5 gap deviate relatively significantly from those of the other gaps (and the corresponding earthquake took place outside the spatial location of the gap), it is not included in the following analysis. For the other five corresponding earthquakes, dynamic T prediction is performed using $T0$ = 500, 600, and 700 days. That way, the predicted occurrence time can be corrected dynamically (every 100 days). Table 2 lists the dynamic prediction results for the occurrence times of earthquakes corresponding to the five seismic gaps (No. 1–4 and No. 6). According to Table 2 when forecasting is started at $T0$ = 500 days, the predicted occurrence time T is 277–505 days (9–17 months).

The average is approximately 379 days (13 months). Considering $T0$ = 600 days, the occurrence time T is within the 177–405 days (6–14 months) range, with an average of 279 days (about 9 months). Finally, when $T0$ = 700 days, the occurrence time T is predicted to be 77–305 days (3–10 months). The average is approximately 179 days (6 months). The predicted occurrence time shortens gradually. The average time reduces from about 16 months (1.3 years) to about 6 months (0.5 years).

Table 2. Dynamic prediction results of the occurrence times of earthquakes corresponding to the five seismic gaps.

Earthquake ID	$T0$ = 400 Days T (Day/Month)	$T0$ = 500 Days T (Day/Month)	$T0$ = 600 Days T (Day/Month)	$T0$ = 700 Days T (Day/Month)
No. 1	419/14	319/11	219/7	119/4
No. 2	573/19	473/16	373/12	273/9
No. 3	377/13	277/9	177/6	77/3
No. 4	605/20	505/17	405/14	305/10
No. 6	423/14	323/11	223/7	123/4
Average	479/16	379/13	279/9	179/6

$T0$: start of forecasting; T: predicted occurrence time.

Among the five earthquakes in Table 2, four took place after $M \geq 4.0$ earthquakes ended the corresponding seismic gaps, whereas one of them directly ended the seismic gap. Actually, when the earthquake occurrence time is predicted using the proposed method, it is not necessary to consider whether the seismic gap has ended or not. As long as the corresponding earthquake has not yet occurred, dynamic correction can continue. The predicted occurrence time can be shortened until it is close to the predicted earthquake.

Therefore, based on the analysis results, if forecasting begins once the $M \geq 4.0$ seismic gap is formed ($T0$ = dT = 400 days), and dynamic correction is performed every 100 days (or at other intervals), the gap can be used as a predictive index on a time scale of about 1–0.5 years or less.

Hypocenter prediction: It is normally located inside or at the margin of the spatial location of the seismic gap. In this paper, the six seismic gap images can be adopted to predict earthquakes mainly in regions inside or at the boundary of the western Sichuan block (Figure 6).

Magnitude (intensity) prediction: There are certain statistical correlations between the following parameters: the magnitudes of initial earthquakes surrounding the spatial location of the seismic gap, the quiet period and semi-major-axis length of the gap, and the magnitudes of future earthquakes. The findings of Qu et al. [7] on seismic gaps in mainland China suggested that when the magnitudes of initial earthquakes surrounding the spatial location of a seismic gap are roughly M4.0, it is possible to predict $M > 7.0$ earthquakes. In addition, according to Lu et al. [10], for the seismic gaps in the central and southern sections of the North–South seismic belt, the relationship between the quiet period, the semi-major-axis length, and the predicted magnitude is given as follows: $M = 0.0965\lg T$ (month) + 4.8300 ± 1.6342 and $M = 0.8832\lg L$ (km) + 4.3670 ± 1.8046, where M denotes the predicted magnitude, T is the quiet period of the seismic gap, and L denotes the semi-major-axis length of the seismic gap. By substituting the average quiet period (19 months, Table 1) and the average semi-major-axis length (987 km, Table 1) of the six seismic gaps examined in this paper into the above equation, the predicted magnitudes are M6.2 and M7.0. The results are basically consistent with the magnitude $M \geq 6.7$ in the present study. Overall, the $M \geq 4.0$ seismic gap images in the study area can be utilized as predictive indexes for $M \geq 6.7$ strong earthquake occurrence.

5. Discussion and Conclusions

In the present research, seismic gaps are identified as the periods with no occurrence of $M \geq 4.0$ earthquake for d$T \geq 400$ days. After examining all records in the Sichuan–Yunnan–Tibet–Qinghai junction area on the southeastern margin of the Tibetan Plateau in 1970–2022, a total of six $M \geq 4.0$ seismic gaps are identified. Spatio-temporal images of the seismic gaps show similar characteristics and demonstrate spatial overlapping and statistical significance. The quiet periods of the six seismic gaps lie between 419 and 777 days (that is, 14–26 months). The average time is approximately 580 days (19 months). Their spatial dimensions and semi-major-axis directions (all in the NNW direction) are basically similar. The semi-major-axis and semi-minor-axis lengths are 880–1050 km and 500–570 km, respectively, with average values of approximately 987 km and 533 km, respectively.

After each seismic gap ended, $M \geq 6.7$ earthquakes occurred either inside or at the margin of its spatial location. The correspondence rate is 100%. Five earthquakes occurred within the spatial location of the gap (83%), while one was at the margin (17%). Case analysis revealed that, for the study area, $M \geq 4.0$ seismic gap images are of high significance in predicting $M \geq 6.7$ strong earthquakes. Occurrence time prediction: If the time of seismic gap formation ($T0$ = dT = 400 days) is taken as the start time of forecasting, and dynamic prediction is done at 100-day intervals, the seismic gap images can act as a predictive index on a time scale of about 1–0.5 years or less. Hypocenter prediction: It is within or at the margins of the spatial locations of the gaps, mainly inside and within the boundary of the western Sichuan block. Magnitude prediction: $M \geq 6.7$ strong earthquakes can be predicted. The above is the outcome of a retrospective statistical analysis of earthquakes, providing only a fundamental statistical understanding. Further testing is necessary to determine the practical effectiveness of the results in predicting future earthquakes.

The concept of seismic gaps, analyzed and discussed in this study, refers to the occurrence of reduced minor earthquake activity around the hypocenter or a sudden decrease before a strong earthquake. This phenomenon is also known as seismic quiescence, indicating a change in the seismic activity within and around the hypocenter. Seismic quiescence preceding strong earthquakes holds the potential for facilitating medium and short-term earthquake predictions and is considered the most reliable precursor by seismologists, generating widespread attention [23–32]. Seismic gaps are commonly attributed to variations in rupture strength within complex seismogenic faults. Initially, low-intensity fault zones experience small background earthquakes due to tectonic stress, while high-intensity fault zones become blocked, resulting in gaps in seismic activity. Kanamori [33] proposed the earthquake asperity model, utilizing the bimodal distribution of sub-fault strengths. Scholz [34] suggested dilatancy hardening, and Wyss [24] linked seismic quiescence to stress relaxation related to precursory slip, to explain this phenomenon. Mei [35] presented a model of an inhomogeneous strong body, considering differences and interactions of medium properties inside and outside the hypocenter, to elucidate the physical mechanisms behind abnormal seismic activity patterns (seismic gaps) preceding strong earthquakes.

Mori and Kawamura [36] employed numerical computer simulations using a one-dimensional spring-block (Burridge-Knopoff) model to investigate the spatiotemporal distribution of earthquakes. They observed that the frequency of smaller events gradually increased before a main shock, but there were very few small events in close proximity to the epicenter. The presence and characteristics of this donut-shaped short-term quiescence depended on the extent of frictional instability in the model. Lu et al. [37] utilized a 3D finite-element model to simulate the spatial distribution features of rock fractures and small earthquakes preceding strong earthquakes. Their findings suggested that randomly distributed cracks surrounding inclusions played a crucial role in the formation of small seismic gaps, belts, and clusters of earthquakes. Ma et al. [38] proposed that "creep sliding" along the fault zone before a large earthquake could be the potential mechanism for seismic quiescence based on experimental results of acoustic emission during rock deformation. Thus, seismic gaps are interpreted as regional complex fault systems or seismogenic regions existing in an unstable or critical state. As stress accumulates, the likelihood of a strong earthquake occurring in these gaps in the future increases.

Identifying seismic gaps commonly involves the utilization of epicenter distribution maps and monitoring temporal changes in earthquake frequency, particularly the interval time. The above are only retrospective statistical analysis results of earthquake records. Hence, merely basic statistical understanding is presented here. The associated physical mechanisms (or models) and quantitative analyses require further studies. Whether the research results can be effectively adopted in actual earthquake prediction has to be further validated.

The spatio-temporal images of the six seismic gaps are very similar, and the gaps show a high degree of spatial overlapping, which indicate remarkable statistical and predictive significance. In recent years, artificial intelligence (AI) tools, such as machine learning, are employed in earthquake prediction [39–42]. A key point is to establish sample datasets and feature parameters for machine learning to train and test the earthquake prediction models. The proposed parameters of the seismic gap images and their spatio-temporal characteristics can, to a certain extent, provide useful sample data for the research and application of AI in related fields.

Author Contributions: Conceptualization, Y.S. and X.Z.; methodology, X.Z. and Y.S.; software, X.Z. and G.W.; validation, X.Z.; formal analysis, X.Z.; investigation, Y.S. and X.Z.; resources, X.Z.; data curation, X.Z. and Y.S.; writing—original draft preparation, X.Z. and Y.S.; writing—review and editing, X.Z. and G.W.; visualization, G.W. and X.Z.; supervision, Y.S. All authors have read and agreed to the published version of the manuscript.

Funding: This research was funded by the National Key R&D Program of China (2021YFC3000705-08).

Institutional Review Board Statement: Not applicable.

Informed Consent Statement: Informed consent was obtained from all subjects involved in the study.

Data Availability Statement: The catalog used in this study is The National Small Earthquake Catalog published by the China Earthquake Networks Center.

Acknowledgments: We thank Wessel et al. for the Generic Mapping Tools (GMT) for plotting some of the figures [43]. We also thank three anonymous reviewers for their thoughtful and constructive comments on an earlier draft.

Conflicts of Interest: All the authors listed certify that they have no involvement in any organization or entity with any financial interests (including honoraria; educational grants; participation in speakers' membership, bureaus, consultancies, stock ownership, employment, or other equity interest; and patent-licensing arrangements or expert testimony) or nonfinancial interests (including professional or personal relationships, knowledge or beliefs, and affiliations) in the subject materials or matter discussed.

References

1. Fedotov, S.A. Regularities of the distribution of strong earthquakes in Kamchatka, the Kuril Islands, and northeastern Japan. *Phys. Earth Acad. Sci.* **1965**, *36*, 66–93.
2. Mogi, K. Two kinds of seismic gaps. *Pure Appl. Geophys.* **1979**, *117*, 1172–1186. [CrossRef]
3. Mei, S.R. Seismicity in China. *Chin. J. Geophys.* **1960**, *9*, 1–19. (In Chinese)
4. Lu, Y.Z.; Shen, J.W.; Song, J.G. Seismic gaps and imminent earthquakes. *Acta Seismol. Sin.* **1982**, *4*, 327–336.
5. Lu, Y.Z.; Wang, W.; Shen, J.W. Seismic gaps and imminent earthquakes (continued). *Acta Seismol. Sin.* **1983**, *5*, 129–144.
6. Rong, Y.; Jackson, D.D.; Kagan, Y.Y. Seismic gaps and earthquakes. *J. Geophys. Res.* **2003**, *108*, 2471–2485. [CrossRef]
7. Qu, Y.J.; Wang, H.T.; Wu, C.D.; Feng, J.G. Analysis on statistic characteristics of seismic gap in Chinese mainland. *Acta Seismol. Sin.* **2010**, *32*, 544–556.
8. Liu, Y.H.; Zhao, G.M.; Wu, Z.H.; Li, Y.H.; Ma, D.; Jian, Y. Application of spatial database technology and seismic gap method to seismic hazard analysis around south-eastern Tibetan Plateau. *J. Geomech.* **2014**, *20*, 255–273.
9. Xue, Y.; Liu, J.; Liu, S.Q.; Wang, Y.Y.; Yang, W. Characteristics of M_S8.1 and M_S7.5 seismic activity in Nepal in 2015. *Chin. Sci. Bull.* **2015**, *60*, 3617–3626.
10. Lu, J.; Song, M.Q.; Zhou, L.Q.; Shao, Z.G.; Xu, F.K.; Cha, X.H.; Li, J. Statistical characteristics of seismic gaps and seismic belts based on earthquake cases in China. *Earthquake* **2016**, *36*, 22–34.

11. Zhang, B.; Zhang, H.; Feng, J.G.; Wang, P.T. Evolution process analysis of seismic gaps of different magnitudes before the 2017 Jiuzhaigou M7.0 earthquake. *Earthq. Res. China* **2018**, *34*, 765–771.
12. Prasath, R.A.; Ajay, P.; Singh, S. Earthquakes in the Garhwal Himalaya of the Central Seismic Gap: A study of historical and present seismicity and their implications to the seismotectonics. *Pure Appl. Geophys.* **2019**, *176*, 4661–4685. [CrossRef]
13. Wang, X.; Song, M.; Chen, H. Statistical analysis of seismic gaps in North China. *Earthquake* **2019**, *39*, 187–195.
14. Petrillo, G.; Rosso, A.; Lippiello, E. Testing of the seismic gap hypothesis in a model with realistic earthquake statistics. *J. Geophys. Res. Solid Earth* **2022**, *127*, e2021JB023542. [CrossRef]
15. Hajra, S.; Hazarika, D.; Shukla, V.; Kundu, A.; Pant, C.C. Stress dissipation and seismic potential in the central seismic gap of the north-west Himalaya. *J. Asian Earth Sci.* **2022**, *239*, 105432. [CrossRef]
16. Teng, C.T.; Chang, Y.M.; Chang, Y.M.; Hsu, K.L.; Fan, F.T. On the tectonic stress field in China and its relation to plate movement. *Phys. Earth Planet. Inter.* **1979**, *18*, 257–435. [CrossRef]
17. Zhang, P.Z.; Deng, Q.D.; Zhang, G.M. Strong earthquake activity and active blocks in mainland China. *Sci. China* **2003**, *33* (Suppl. S1), 12–20.
18. Song, F.M.; Wang, Y.P.; Yu, W.X. *The Xiaojiang Fault Zone*; Seismological Press: Beijing, China, 1998; pp. 209–232.
19. Su, Y.J.; Qin, J.Z. Relationship between strong seismicity in the Sichuan-Yunnan area and regional neotectonics. *Earthq. Res. China* **2001**, *17*, 24–34.
20. Su, Y.J.; Li, Y.L.; Li, Z.H. Analysis of minimum complete magnitude of earthquake catalog in Sichuan-Yunnan region. *J. Seismol. Res.* **2003**, *26* (Suppl. S1), 10–16.
21. Mignan, A.; Jiang, C.; Zechar, J.D.; Wiemer, S.; Wu, Z.; Huang, Z. Completeness of the mainland China earthquake catalog and implications for the setup of the China earthquake forecast testing center. *Bull. Seism. Soc. Am.* **2003**, *103*, 845–859. [CrossRef]
22. Shi, X.Y.; Wang, X.Q.; Qiu, Y.R.; Yuan, X. Analysis of the minimum magnitude of completeness for earthquake catalog in China Seismic Experimental Site. *Chin. J. Geophys.* **2020**, *63*, 3683–3697. (In Chinese)
23. Habermann, R.E. Precursory seismic quiescence: Past, present and future. *Pure Appl. Geophys.* **1988**, *126*, 79–318. [CrossRef]
24. Wyss, M.; Habermann, R.E. Precursory seismic quiescence. *Pure Appl. Geophys.* **1988**, *126*, 319–332. [CrossRef]
25. Wyss, M.; Martirosyan, A.H. Seismic quiescence before the M7, 1988, Spitak earthquake, Armenia. *Geophys. J. Int.* **1998**, *134*, 329. [CrossRef]
26. Kisslinger, C. An experiment in earthquake prediction and the 7 May 1986 Andreanof Islands earthquake. *Bull. Seism. Soc. Am.* **1988**, *78*, 218–229.
27. Wiemer, S.; Wyss, M. Seismic quiescence before the Landers (M = 7.5) and Big Bear (M = 6. 5) 1992 earthquakes. *Bull. Seism. Soc. Am.* **1994**, *84*, 900–916.
28. Kato, N.; Ohtake, M.; Hirasawa, T. Possible mechanism of precursory seismic quiescence: Regional stress relaxation due to preseismic sliding. *Pure Appl. Geophys.* **1997**, *150*, 249–267. [CrossRef]
29. Katsumata, K.; Kasahara, M. Precursory seismic quiescence before the 1994 Kurile earthquake (Mw = 8.3) revealed by three independent seismic catalogs. *Pure Appl. Geophys.* **1999**, *155*, 443–470. [CrossRef]
30. Huang, Q.; Sobolev, G.A.; Nagao, T. Characteristics of the seismic quiescence and activation patterns before the M = 7.2 Kobe earthquake, 17 January 1995. *Tectonophysics* **2001**, *337*, 99–116. [CrossRef]
31. Ogata, Y. Space-time model for regional seismicity and detection of crustal stress changes. *J. Geophys. Res. Atmos.* **2004**, *109*, 23. [CrossRef]
32. Wu, Y.; Chiao, L. Seismic quiescence before the 1999 Chi-Chi, Taiwan, Mw 7.6 earthquake. *Bull. Seism. Soc. Am.* **2006**, *96*, 321–327. [CrossRef]
33. Kanamori, H. The nature of seismicity patterns before large earthquakes. In *Earthquake Prediction*; Simpson, D.W., Richards, P.G., Eds.; American Geophysical Union: Washington, DC, USA, 1981; pp. 1–19.
34. Scholz, C.H. Mechanisms of seismic quiescences. *Pure Appl. Geophys.* **1988**, *126*, 701–718. [CrossRef]
35. Mei, S.R. On the physical model of earthquake precursor fields and the mechanism of precursors' time-space distribution (III)—Anomalies of seismicity and crustal deformation and their mechanisms when a strong earthquake is in preparation. *Acta Seismol. Sin.* **1996**, *9*, 223–234. [CrossRef]
36. Mori, T.; Kawamura, H. Simulation study of the one-dimensional Burr-idge-Knopoff model of earthquakes. *J. Geophys. Res.* **2006**, *111*. [CrossRef]
37. Lu, Y.Z.; Ye, J.D.; Jiang, C.; Liu, J. 3Dnumerical simulation on the mechanism of precursory seismicity pattern before strong earthquake in China. *Chin. J. Geophys.* **2007**, *50*, 499–508. (In Chinese)
38. Ma, S.L.; Jiang, H.K.; Hu, X.Y.; Ba, J. A discussion on mechanism for seismic quiescence before large earthquakes based on experimental results of acoustic emission. *Seismol. Geol.* **2004**, *26*, 426–435. (In Chinese)
39. Huang, J.P.; Wang, X.A.; Zhao, Y.; Xin, C.; Xiang, H. Large earthquake magnitude prediction in Taiwan based on Deep Learning Neural Network. *Neural Netw. World* **2018**, *28*, 149–160. [CrossRef]
40. Mignan, A.; Broccardo, M. Neural network applications in earthquake prediction (1994–2019): Meta-analytic and statistical insights on their limitations. *Seismol. Res. Lett.* **2020**, *91*, 2330–2342. [CrossRef]
41. Mousavi, S.M.; Gregory, C.B. Deep-learning seismology. *Science* **2022**, *377*, eabm4470. [CrossRef]

42. Wang, J.H.; Jiang, H.K. A review of machine learning earthquake prediction based on earthquake observation data. *J. Seismol. Res.* **2023**, *46*, 173–187. Available online: https://link.cnki.net/doi/10.20015/j.cnki.issn1000-0666.2023.0022 (accessed on 28 June 2023).
43. Wessel, P.; Luis, J.F.; Uieda, L.; Scharroo, R.; Wobbe, F.; Smith, W.H.F.; Tian, D.D. The Generic Mapping Tools Version 6. *Geochem. Geophys. Geosyst.* **2019**, *20*, 5556–5564. [CrossRef]